water

MDPI

Article

Influence of Humic Acid on the Transport and Deposition of Colloidal Silica under Different Hydrogeochemical Conditions

Jingjing Zhou [1,2], Wenjing Zhang [1,2,*], Dan Liu [1,2], Zhuo Wang [1,2] and Shuo Li [1,2]

[1] Key Laboratory of Groundwater Resources and Environment, Ministry of Education, Jilin University, Changchun 130021, China; zhoujingjing7777@163.com (J.Z.); 18643117873@163.com (D.L.); wz18088684176@163.com (Z.W.); fantasy_shuo@sina.com (S.L.)

[2] College of Environment and Resources, Jilin University, Changchun 130021, China

* Correspondence: zhwenjing@jlu.edu.cn; Tel.: +86-43-8850-2606

Academic Editor: Pieter J. Stuyfzand

Received: 26 October 2016; Accepted: 20 December 2016; Published: 28 December 2016

Abstract: The transport and deposition of colloids in aquifers plays an important role in managed aquifer recharge (MAR) schemes. Here, the processes of colloidal silica transport and deposition were studied by displacing groundwater with recharge water. The results showed that significant amounts of colloidal silica transport occurred when native groundwater was displaced by HA solution. Solution contains varying conditions of ionic strength and ion valence. The presence of humic acid could affect the zeta potential and size of the colloidal silica, which led to obvious colloidal silica aggregation in the divalent ion solution. Humic acid increased colloidal silica transport by formation of non-adsorbing aqueous phase silica–HA complexes. The experimental and modeling results showed good agreement, indicating that the essential physics were accurately captured by the model. The deposition rates were less than 10^{-8} s^{-1} in deionized water and monovalent ion solution. Moreover, the addition of Ca^{2+} and increase of IS resulted in the deposition rates increasing by five orders of magnitude to 10^{-4} s^{-1}. In all experiments, the deposition rates decreased in the presence of humic acid. Overall, the promotion of humic acid in colloidal silica was strongly associated with changes in water quality, indicating that they should receive greater attention during MAR.

Keywords: colloidal silica; humic acid (HA); managed aquifer recharge (MAR); transport and deposition; sand columns

1. Introduction

Managed aquifer recharge (MAR) projects, which play a significant role in controlling environmental–geological problems and treating drinking water, have been conducted worldwide [1,2]. However, the hydrogeochemical characteristics of MAR water are different from those of groundwater, which can perturb the native condition of an aquifer, resulting in release of natural colloids into the groundwater [3]. The released colloids are then transported and deposited with water flow during MAR, which can lead to physical clogging [4]. Additionally, it is now well accepted that colloids play a significant role in pollutant transport, soil fertility, and aquifer structure [5,6].

Aquifer environments always contain mineral colloids, among which colloidal silica is the most abundant form [7,8]. Colloidal silica plays an important role in determining the fate of contaminants in subsurface environments, either as adsorbents or as mobile carriers [9]. Decreased permeability of a porous medium may occur because of colloidal matter deposition. Mineral colloids and humic acid (HA) often co-exist, which results in electrostatic interactions. The MAR water from surface water always contains some HA, which may be released during MAR. Hence, the dissolved HA in

groundwater inevitably increases during MAR. Previous studies have indicated the importance of the presence of dissolved HA to the mobility of colloids [10–13]. Accordingly, understanding the effects of HA on transport of colloidal silica in porous media under different hydrogeochemical conditions is important to preventing groundwater pollution and contamination removal during MAR.

This study was conducted to compare the transport and deposition of colloidal silica with and without humic acid under different hydrochemical (ionic strength and ion valence) conditions in sand packed columns. Humic acid was used as a model natural organic matter and KCl and $CaCl_2$ were used to adjust the ionic strength and ion valence. The COMSOL Multiphysics platform was then used to simulate the experimental results using the advection dispersion equation and to simulate the deposition process by an equilibrium isotherm, a first-order kinetic process, or nonlinear kinetics [14,15].

2. Materials and Methods

2.1. Colloidal Silica

Silica nanoparticles have been listed by the Organization for Economic Co-operation and Development (OECD) as a representative manufactured nanomaterial for safety testing [16]. Silica nanoparticles are good candidates for modeling of natural colloidal silica because the properties of SiO_2 are similar to those of natural mineral colloids [17]. In this study, the colloids used were mono-dispersed silica microspheres (Polysciences Inc., Philadelphia, PA, USA). The colloidal silica was provided in a 5.59% aqueous dispersion and diluted to achieve 100 mg/L stock solution, which was later diluted to 20 mg/L for transport experiments. The concentration of colloidal silica was 20 mg/L in aquifer recharge research of Wang et al. [18]. The 100 mg/L silica dispersions were sonicated for 15 min prior to dilution to disaggregate and disperse the particles. The particle size, zeta potential and concentration of colloidal silica was measured using a Malvern Zetasizer (Nano ZS, Malvern, UK). Particle size and zeta potential were tested three times.

2.2. Preparation of Porous Media

Sands were used without any specific treatment as the column packing material. The natural sands (Aggregate Industries, Leicestershire, UK) consisted of 99.7% silica and less that 0.3% other oxides (data from the manufacturer). The grain size distribution was D50 = 0.42 mm, D60/D10 = 1.4.

2.3. Electrolyte Solutions

Based on the variety of MAR water quality characteristics, monovalent ion solution, divalent ion solution and mixed solution (ion solution and divalent ion) were considered in the experiments. KCl (aq) and $CaCl_2$ (aq) were used to control cation types, and HA, a primary component of NOM in freshwater systems [19,20], was used to study the role of natural organic matter on colloidal silica transport. Suwannee River HA (SRHA) standard II from the International Humic Substance Society that has been widely employed in many previous studies as a kind of natural organic matter [20–22], was used in this study. A 20 mg dry HA was introduced to 100 mL of deionized water and sonicated for 30 min to disperse the particles, after which it was stored at 10 °C. The concentration in the experiment was 10 mg/L according to research by Liu et al. [23].

2.4. Column Experiments

All experiments were conducted using Plexiglas columns with a length of 10 cm and an internal diameter of 3 cm. The column was dry-packed with sand and polyethylene meshes were placed at both ends of the column to prevent the sands from leaking. The effective length of sand in the columns was 6.5 cm, and average pore volume was 12 mL. The column packing porosity for each experiment was determined to be 0.25–0.30 based on the measured column quality.

A schematic of the equipment is shown in Figure 1. A peristaltic pump was used to pump an aqueous particle suspension through the packed column at a constant speed. To prevent air bubbles, the packed column was set up vertically and saturated with deionized water from bottom to top. The pH of outflow from the column was measured using a pH flow cell connected to a Metrohm Aquatrode Electrode, and values were collected continuously using a Datataker DT80 data logger. Particle concentrations, size and zeta potential in the column effluent were monitored using a Malvern Zetasizer (Nano ZS, Malvern Instruments, Malvern, UK).

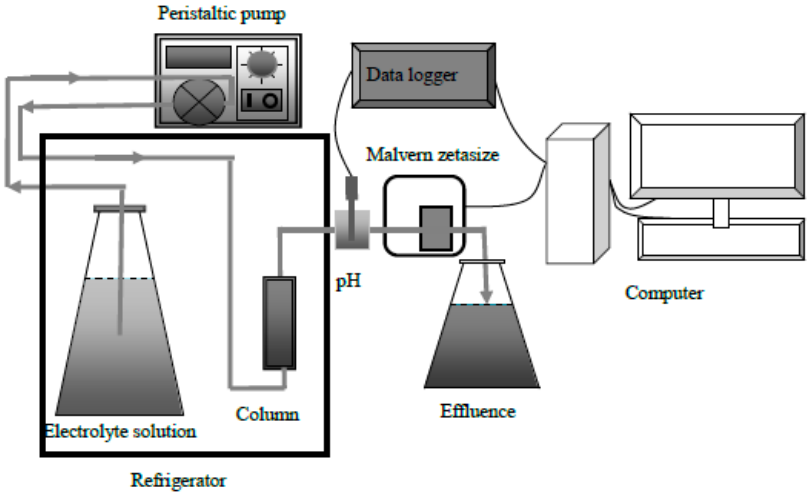

Figure 1. Schematic of the experiment.

Each experiment contains two stages. Stage one: the packed column was first saturated with deionized water over 24 h at a low flow rate (0.2 mL/min) to dislodge air bubbles. This pretreatment ensured stable conductivities and pH at the column outlet. The ion strength (IS) of groundwater is commonly lower than that of MAR water. Hence, the deionized water was selected to represent native groundwater. Stage two: the colloidal silica suspension was injected into the packed column at a steady flow rate of 0.36 mL/min corresponding to a Darcy velocity of around 0.05 cm/min. The backwash was not performed. All experiments were conducted at a natural groundwater temperature of 10 °C. Chloride in the form of sodium chloride (NaCl) was selected as the nonreactive tracer.

Colloidal silica transport experiments were conducted under different ion component conditions, and every ion component contained two conditions: in the absence and presence of HA. Four different series of column experiments were performed;

(1) Colloidal silica transport experiments in deionized water;
(2) Colloidal silica transport experiments in the presence of monovalent ion (KCl, 0.01 mol/L);
(3) Colloidal silica transport experiments in the presence of divalent ion ($CaCl_2$, 0.0025 mol/L and 0.05 mol/L);
(4) Colloidal silica transport in the presence of monovalent ion and divalent ion (KCl, 0.01 mol/L and $CaCl_2$, 0.0025 mol/L).

2.5. Mathematical Model

The mathematical model was developed to recreate the experimental breakthrough curves to describe the processes of colloid transport and deposition in one-dimensional settings to enable comparison of the experimental data. Colloid transport was described as follows using the advection–dispersion equation with terms for colloid deposition at pore constrictions:

$$\frac{\partial C}{\partial t} + \frac{\rho_B}{\theta}\frac{\partial F_d}{\partial t} = \frac{\partial}{\partial t}\left[D\frac{\partial C}{\partial x} - vC\right] \quad (1)$$

where, C (M/L^3) is the colloidal silica concentration in the aqueous phase, t (T) is the time, F_d (M/M) is the colloidal silica concentrations retained by deposition on grain surfaces, v (L/T) is the mean pore water velocity, D (L^2/T) is the hydrodynamic dispersion coefficient from the tracer experiment (6×10^{-11} m^2/s), θ (-) is the porosity, and ρ_B (M/L^3) is the bulk density of the porous media.

In the absence of colloid inactivation or degradation, the following equation was used to describe processes of colloid deposition/detachment models:

$$\frac{\rho_B}{\theta}\frac{\partial F_d}{\partial t} = k_d \psi_d C - \frac{\rho_B}{\theta} k_{\mathrm{det}} F_d \quad (2)$$

where k_d (1/T) and k_{det} (1/T) are the first-order deposition and detachment rate from the porous media, respectively, k_d was computed according to Syngouna and Chrysikopoulos [24], and ψ_d is a dimensionless colloid deposition function. The value of ψ_d was equal to 1 for clean-bed conditions.

The value of ψ_{d} is a linear function of F_d:

$$\psi_d = 1 - F_d / F_d^{\max} \quad (3)$$

where, $F_d^{\max}$ is the solid-phase concentration of attached colloids. In this study, it was assumed that colloid deposition primarily occurred at the column inlet.

Simulations were performed using COMSOL Multiphysics. For the simulation discussed below, a zero flux boundary condition was used at the inlet, and a concentration gradient of zero was specified at the outlet. An initial condition of no suspended colloids in solution and a fixed uniform concentration of initially deposited colloids in the simulation domain were used.

3. Results and Discussion

3.1. Characterization of Colloidal Silica

Four different series of colloidal silica transport experiments were conducted in the present study (Table 1). These included experiments in the presence of divalent ions including two different concentrations of $CaCl_2$ (0.0025 mol/L and 0.005 mol/L).

Table 1. Experimental conditions and results for column tests under different hydrochemical conditions.

Group	TEST NO.	SiO_2 (ppm)	HA (ppm)	KCl (mol/L)	$CaCl_2$ (mol/L)	PH	IS (M)	Peak (%)	R
1	T1	10	0	0	0	6~7	<0.0005	100	1
2	T2	10	0	0.01	0	6~7	0.013	100	1.5
3	T3	10	0	0	0.0025	6~7	0.0093	70	2.3
	T4	10	0	0	0.005	6~7	0.013	32	15
4	T5	10	0	0.01	0.0025	6~7	0.0225	69	4.6
1	T1′	10	10	0	0	6~7	<0.0005	100	1
2	T2′	10	10	0.01	0	6~7	0.013	100	1.25
3	T3′	10	10	0	0.0025	6~7	0.0093	85	2
	T4′	10	10	0	0.005	6~7	0.013	38	8
4	T5′	10	10	0.01	0.0025	6~7	0.0225	68	3

Notes: R is retardation coefficient calculated according to the breakthrough curve; Peak is the peak value of colloid recovered in the effluent after the colloidal silica breakthrough curve reached a plateau.

Colloidal silica is one of the soil mineral precipitate colloids in the subsurface environment. Ions and humic acid can control the sizes and zeta potential of colloidal silica. In this study, the zeta potential and size of colloidal silica were detected under different hydrogeochemical conditions (Figures 2 and 3).

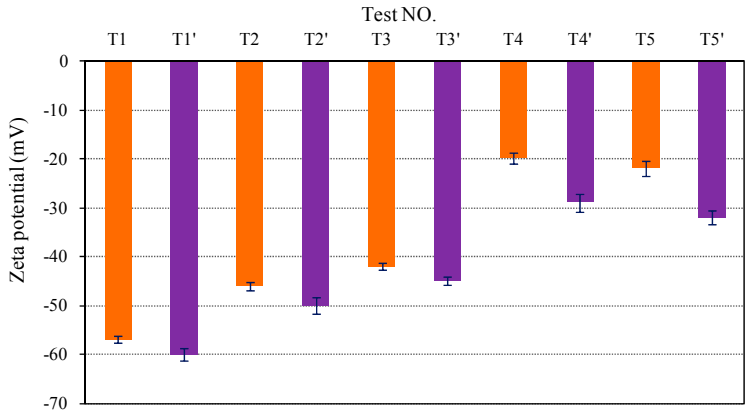

Figure 2. Colloidal silica zeta potential under different conditions.

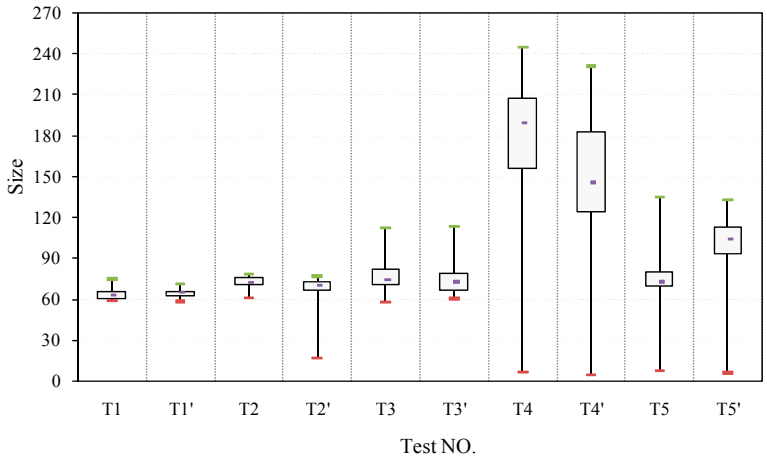

Figure 3. Colloidal silica size distributions under different conditions. Colloidal silica particle size is the value of the normalized column effluent suspension after two pore volumes.

The zeta potential of colloidal silica was negatively charged under all conditions (Figure 2). When compared to those without HA, more negative zeta potential was observed in the colloidal silica suspension with HA. The zeta potential increased from −57 mV to −20 mV in the absence of HA with a similar trend to that observed in the presence of HA. The zeta potential of colloidal silica in the presence of monovalent ion exhibited a more negative charge than colloidal silica in the presence of divalent ion. These results confirmed that divalent ion Ca^{2+} changes the surface properties of the colloidal silica significantly. Phenolic groups of HA can by attracted by negatively charged colloidal silica surface and carboxylic dissociated groups of HA could be oriented to the outside yielding a more negative global charge of colloidal silica as zeta potential results showed. More negatively charged colloidal silica after the addition of HA has also been observed in other previous studies [25,26]. For high concentrations of Ca^{2+} (T4 and T4′) and mixing ion (T5 and T5′) conditions, the measured zeta potentials differ significantly in the presence and absence of HA.

The mean size of colloidal silica varied from 61 to 156 nm, and the mean size and size range increased with ion concentration and ion valence (Figure 3). These results suggest that colloidal aggregation occurred in high IS and ion valence. From T1 to T3, only a very little increase in size could be observed, and the difference in colloidal silica size with and without HA was not significant. As the ion concentration and addition of divalent ion increased, the stability of colloidal silica decreased and the particle size range increased. The increased size of colloidal silica in high IS (Ca^{2+}) was also observed by Wang et al. [18], and the increased colloidal silica particle may form colloidal silica-colloidal silica(T4) and colloidal silica-HA-calcium(T4′).

3.2. Colloidal Silica Transport Experiment

3.2.1. Influence of Hydrogeochemical Conditions on Colloidal Silica Transport during MAR

Five colloid experiments (T1–T5) were conducted under different hydrogeochemical conditions (Table 1 and Figure 4). The effluent colloid concentration reached 100% of the initial silica concentration under the deionized water (T1) and monovalent ion solution (T2) conditions, whereas under divalent ion solution (T3), only 70% of the initial concentration was recovered. Moreover, the retardation coefficient of T2 (R = 1.5) and T3 (R = 2.3) was higher than that of T1 (R = 1). These results indicate that deposition of colloidal silica increased with IS, and the influence of divalent ion is significant in the suspension during MAR. These findings are in agreement with the results obtained by Bekhit et al. [14] and Jiang et al. [27].

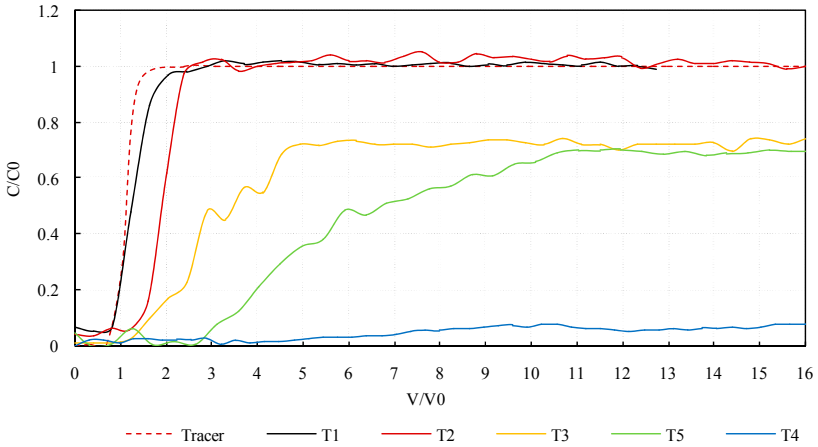

Figure 4. Experimental breakthrough curves for colloidal silica under different hydrogeochemical conditions.

To further reveal the influence of IS and divalent ion, T4 and T5 were conducted. In the T4 test, there was a slow breakthrough and C/C_0 did not reach 10% before 16 V/V_0, which required around 15 pore volumes from the introduction of particles to reach peak concentration. Comparison of T3 with T4 revealed that increasing the ionic strength in the aqueous phase will increase the deposition of colloidal silica. Comparison of T4 with T5 revealed that, although the IS of T5 is high, T5 takes around 4.6 pore volumes to reach the peak C/C_0 of close to 69%. These findings indicate that colloid mobility decreased in the presence of divalent Ca^{2+} in suspensions. These results also clearly demonstrate that the presence of Ca^{2+} has a greater influence on the transport of colloidal silica than IS. The zeta potential became more positive when IS increased and with the addition of Ca^{2+}, with measured zeta potentials in the range of −57 mV to −20 mV. The increase in colloidal silica deposition with increasing ionic strength agrees with the trend of zeta potentials, indicating that increasing ionic strength compresses the electric double layer and decreases layer thickness. Therefore, increasing ionic strength allows the van der Waals attractive forces to dominate (thereby overcoming the electrostatic repulsion forces). The observed high deposition in $CaCl_2$ solutions relative to KCl solutions was consistent with the less negative zeta potentials of colloidal silica in the presence of divalent Ca^{2+} in suspensions.

The transport of colloidal silica in glass bead porous media under relevant IS in both NaCl and $CaCl_2$ solutions has been thoroughly discussed by other researchers in our research team [18]. The results of the present study, which was conducted in sand porous media, are generally in agreement with the results of these previous studies; however, the retardation coefficient and the peak of colloidal silica breakthrough under similar hydrogeochemical conditions differed [18]. In our study, the retardation coefficient was smaller and the peak was higher under low IS conditions, while the retardation coefficient was larger and the peak was lower under high IS conditions. In other words, the change in the colloidal silica breakthrough curve with increasing IS was more obvious in the present

study. One possible explanation for this difference is that the smaller colloidal silica particle size and the more negative zeta potential in the present study may lead to efficient transport of colloidal silica under low IS conditions. Nevertheless, the sand porous media used in our study played an important role in high IS. The surface roughness of sand and glass beads differs, with high surface roughness of sand leading to decreased transport. These findings imply that changes in the colloid size and porous media should receive increased attention in future research.

3.2.2. Influence of HA on Colloidal Silica Transport in Monovalent Ion Solution during MAR

The breakthrough curves and particle sizes of colloidal silicafor when the experiments were conducted in deionized water and monovalent ion solution are shown in Figure 5. The colloidal silica particle size of colloidal silica was unstable before 2 V/V_0. According to a study conducted by Torkzaban et al. [28], changing the solution chemistry from low salinity groundwater to reverse-osmosis water resulted in a significant release of colloids originally deposited on sand. Hence, the sand without any specific treatment may release some particles, leading to changes in particle size. The colloidal silica particle size is the value of the normalized column effluent suspension after two pore volumes as shown in Figure 3. The colloidal silica particle size showed very slight changes in deionized water and monovalent ion solution. Colloidal silica transport was efficient and C/C_0 reached 1 after 3 pore volumes (Figure 5a). The breakthrough curves and colloidal silica particle size varied slightly with and without HA, indicating that HA had only a slight influence on colloidal silica transport in deionized water.

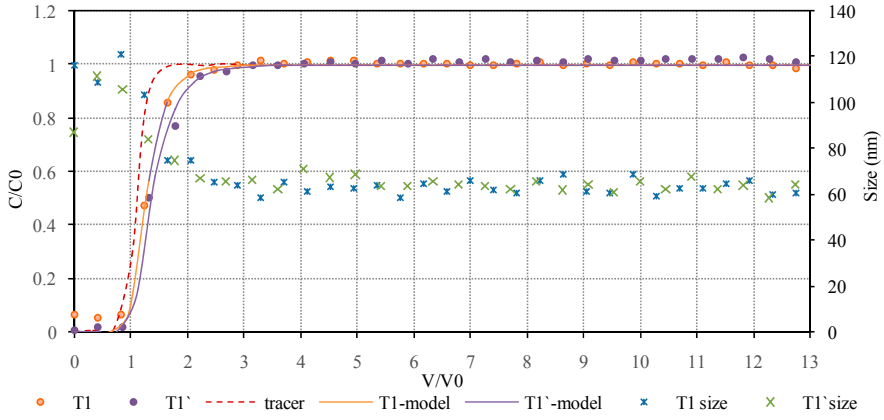

(**a**)

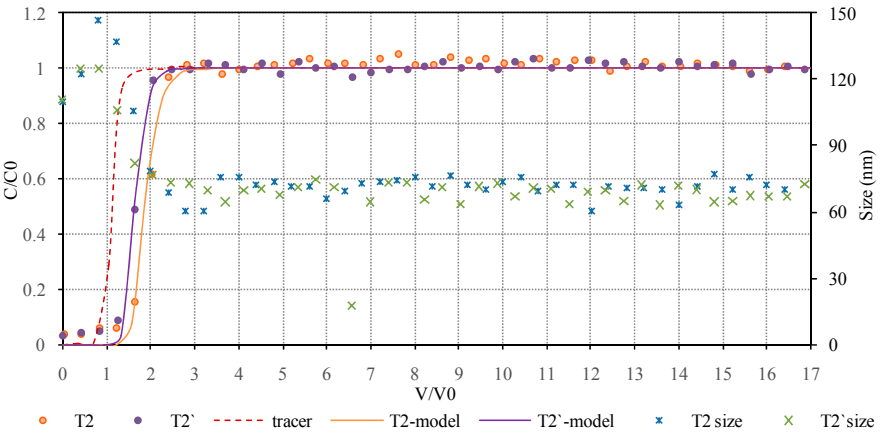

(**b**)

Figure 5. Experimental breakthrough curves for colloidal silica with and without HA in: (**a**) deionized water; (**b**) monovalent ion solution.

Although the C/C_0 could reach 1 in monovalent ion solution, the retardation coefficient decreased by 17% from T2 to T2′ in monovalent ion solution, suggesting that HA led by MAR could promote colloidal silica transport. The zeta potential of colloidal silica is more negative in the presence of HA. Blocking of colloidal silica with HA reduces the formation of silica–silica. The adsorption of HA onto colloidal silica can reach 62% after 2 h [29]. Hence, the potential mechanism for the increased HA transport in the presence of HA is formation of non-adsorbing aqueous silica-HA and increased electrostatic repulsion between silica–HA and sand. HA adsorption onto other colloidal particles was also found in a study conducted by Chen et al. [30]. The increase in mobility of colloidal particles with HA in monovalent ion solution has been observed in previous studies [30,31].

3.2.3. Influence of HA on Colloidal Silica Transport in Divalent Ion Solution during MAR

As shown in Figure 6a,b, breakthrough curves for colloidal silica were obtained with high levels of eluted colloidal silica in the presence of HA. As shown in Figure 6a, the retardation coefficient decreased by 13% and the peak increased by 21% from T3 to T3′. The retardation coefficient decreased and peak increased from T4 to T4′, and the reduced rate of the retardation coefficient (47%) was higher than that from T3 to T3′. These findings not only suggest that HA led by MAR promotes colloidal silica transport, but also that the promotion of HA is efficient in high IS MAR solution because of salt enhanced humic acid adsorption onto colloidal silica. A study by Thio et al. [32] suggested that HA would become more coiled with increased IS. At high IS, the formation of cation bridges was facilitated between HA molecules and cations in solutions. The conformation of HA strands becomes more compact; therefore, the adsorbed layer became more dense with increasing IS. In addition, the amount of HA adsorbed onto the colloidal particles progressively increased with increasing IS through electrostatic interaction and specific adsorption via ligand exchange [29,30]. Consequently, a greater amount of HA was adsorbed onto colloidal silica in high IS solution, leading to enhanced electrostatic and steric hindrance. Saleh, Pfefferle and Elimelech [19] reported decreased aggregation of colloidal particles' nanoparticles in divalent ion solution in the presence of HA.

3.2.4. Influence of HA on Colloidal Silica Transport in Mixed (Monovalent Ion and Divalent Ion) Solution during MAR

Breakthrough curves obtained when the experiments were conducted using mixed solution are shown in Figure 7. Although the peaks of T5 and T5′ were close, the retardation coefficient decreased by 38%. These findings demonstrate that HA can also promote the transport of colloidal silica in mixed solution. The retardation coefficient decreased by 47% from T4 to T4′, which was a greater increase than that in high IS mixed solution. These findings suggest that the influence of divalent ion Ca^{2+} is stronger than that of monovalent ion K^+ on HA absorbed to colloidal silica.

The sand has a high capacity to adsorbing colloidal silica, especially in the presence of Ca^{2+}. These results were likely related to decreasing the affinity of the sand grains for deposition of colloidal silica with the addition of HA. The increased negative zeta potential in the presence of HA can promote the colloidal silica transport. It has also been reported that HA would become more coiled in the presence of divalent cations than monovalent cations [23]. Divalent cations have stronger ability than monovalent cations to promote charge neutralization. Hence, the promotion of HA is stronger under divalent ion conditions. This behavior may be attributed to the HA macromolecules undergoing non-adsorbing complex formation with calcium ions and adsorption onto the colloidal silica (colloidal silica-HA-calcium), which reduces the charge and steric influences of the adsorbed macromolecular layers [20,33]. The finding that the addition of humic acid in salt solution retarded colloids' deposition has been observed in many previous studies [22,31].

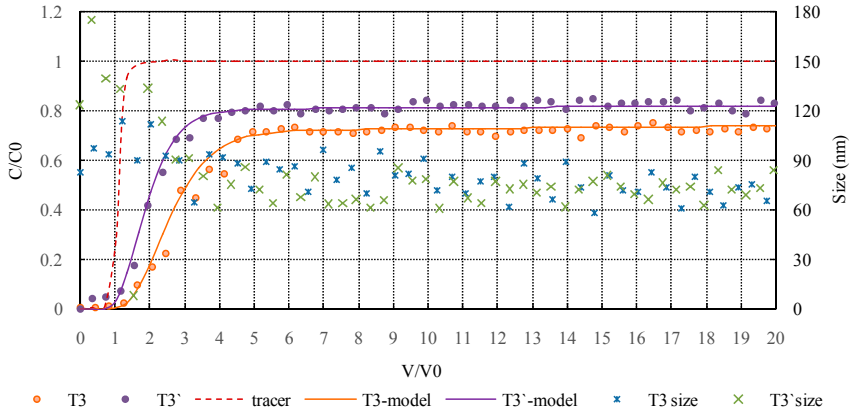

(**a**)

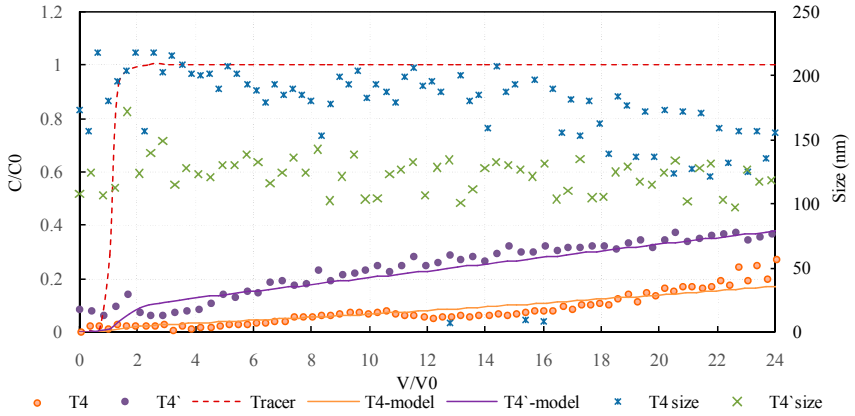

(**b**)

Figure 6. Experimental breakthrough curves for colloidal silica with and without HA in divalent ion solution: (**a**) IS = 0.0093 M; (**b**) IS = 0.013 M.

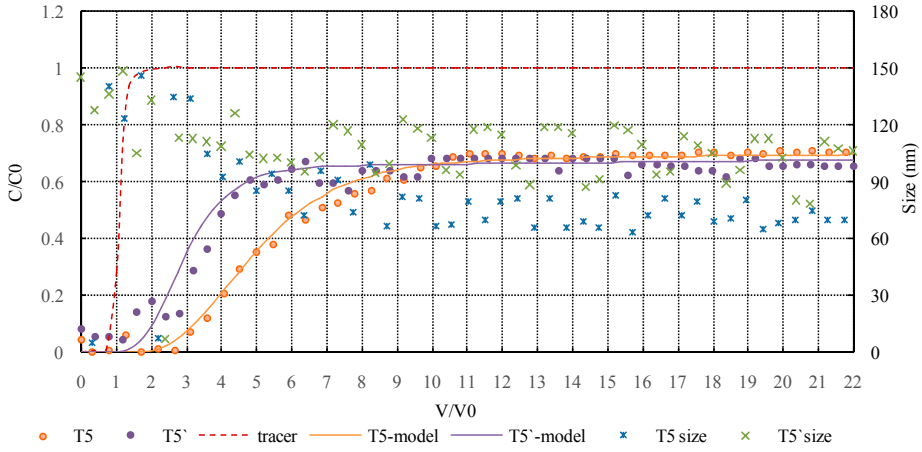

Figure 7. Experimental breakthrough curves for colloidal silica with and without HA in mixed solution.

3.3. Modeling Results and Discussion

The T5′ model breakthrough curve closely matched the experimental data in the later part of the breakthrough curve (after five pore volumes) in Figure 7. However, the T4 and T4′ model breakthrough curve was more deflected to the experimental data than that of the other experiments after five pore

volumes. As shown in Figure 5, the T5 model closely matched the experimental data before five pore volumes. The model results for the rest of the breakthrough curves appeared very efficient for fitting the experimental data, where the modeled breakthrough time and overall trend of the curve were in very good agreement with the experimental data.

The deposition rates of the transport model are presented in Table 2. The deposition rates were all less than 10^{-8} s^{-1} in deionized water and monovalent ion solution. With the addition of Ca^{2+} and the increase of IS, the deposition rates increased by five orders of magnitude to 10^{-4} s^{-1}. In all experiments, the deposition rates decreased in the presence of HA. The deposition rates of undisturbed sandstone observed by Anderson [34], quartz sand observed by Elimelech et al. [35], and glass beads observed by Wang et al. [18] were 9.57×10^{-3} s^{-1}, 1×10^{-3} s^{-1} and 6.43×10^{-5} s^{-1}, respectively, all of which differed from the values of the divalent ion solution and mixed ion solution observed in this study. Hence, with the exception of the ion valence and HA in MAR solution, the characterization of porous media needs to be considered during MAR. Additionally, the deposition rate increased with heterogeneous porous media.

Table 2. Deposition rates used from simulation of colloidal silica.

Test	**T1**	**T2**	**T3**	**T4**	**T5**
k_d **(s^{-1})**	1.83×10^{-9}	9.55×10^{-9}	1.84×10^{-4}	3.64×10^{-4}	2.41×10^{-4}
Test	T1′	T2′	T3′	T4′	T5′
k_d **(s^{-1})**	1.52×10^{-9}	7.64×10^{-9}	1.06×10^{-4}	3.52×10^{-4}	1.88×10^{-4}

4. Conclusions

This study systemically investigated the transport and deposition behaviors of colloidal silica, one of the most popular mineral colloids, in packed sand over series of MAR relevant HA solutions. The transport kinetics of colloidal silica were closely related to that of HA in different IS, ion valence. Increasing the MAR solution IS and ion valence clearly increased the deposition and aggregation of colloidal silica on sand.

The transport of colloidal silica is efficient in low IS and mono-valent ion in the absence and presence of HA; therefore, when the MAR water is injected the promotion of HA is not obvious. Increasing solution ionic strength and cation valence increased the deposition of colloidal silica on the sand. The presence of HA in MAR solutions distinctly reduced the retardation coefficient. Moreover, the presence of HA strongly influenced the zeta potential and size of original groundwater colloidal silica. Colloidal silica aggregation increased in size in divalent ion solution. Additionally, HA increased colloidal silica transport via the improved negative charge and the potential formation of non-adsorbing aqueous phase silica–HA complexes in high IS. The increased transport of colloidal silica by MAR water (containing HA) will increase the risk of colloidal facilitated pollution. Comparison of the fitted and experimentally measured effluent colloid concentrations and associated changes showed good agreement, indicating that the essential physics were accurately captured by the model. Additionally, comparison of the deposition rate with that available in the literature revealed that the characteristics of colloidal silica and porous media need to be considered during MAR. Given that HA are present everywhere in surface water and groundwater, the results of this study highlight the importance of the influence of HA on the transport and deposition of colloidal silica during MAR.

Acknowledgments: This research was funded by the National Natural Science Foundation of China (Grant No. 41472215). The authors thank the journal editors and the reviewers for their valuable comments, which improved the paper considerably. We also thank the staff at the University of Birmingham, United Kingdom, for their warm assistance in the laboratory.

Author Contributions: Wenjing Zhang and Jingjing Zhou conceived and designed the experiments. Jingjing Zhou and Dan Liu performed the experiments and analyzed the data. Wenjing Zhang contributed reagents/materials/analysis tools. The manuscript was prepared by Zhuo Wang and Shuo Li and revised by Wenjing Zhang.

Conflicts of Interest: The authors declare no conflict of interest.

References

1. Zhang, W.J.; Huan, Y.; Yu, X.P.; Liu, D.; Zhou, J.J. Multi-component transport and transformation in deep confined aquifer during groundwater artificial recharge. *J. Environ. Manag.* **2015**, *152*, 109–119. [CrossRef] [PubMed]
2. Maeng, S.K.; Sharma, S.K.; Lekkerkerker-Teunissen, K.; Amy, G.L. Occurrence and fate of bulk organic matter and pharmaceutically active compounds in managed aquifer recharge: A review. *Water Res.* **2011**, *45*, 3015–3033. [CrossRef] [PubMed]
3. Bradford, S.A.; Torkzaban, S.; Leij, F.; Simunek, J. Equilibrium and kinetic models for colloid release under transient solution chemistry conditions. *J. Contam. Hydrol.* **2015**, *181*, 141–152. [CrossRef] [PubMed]
4. Masciopinto, C. Management of aquifer recharge in lebanon by removing seawater intrusion from coastal aquifers. *J. Environ. Manag.* **2013**, *130*, 306–312. [CrossRef] [PubMed]
5. Sen, T.K.; Khilar, K.C. Review on subsurface colloids and colloid-associated contaminant transport in saturated porous media. *Adv. Colloid Interface Sci.* **2006**, *119*, 71–96.
6. Vendelboe, A.L.; Moldrup, P.; Schjonning, P.; Oyedele, D.J.; Jin, Y.; Scow, K.M.; de Jonge, L.W. Colloid release from soil aggregates: Application of laser diffraction. *Vadose Zone J.* **2012**, *11*. [CrossRef]
7. Baumann, T.; Fruhstorfer, P.; Klein, T.; Niessner, R. Colloid and heavy metal transport at landfill sites in direct contact with groundwater. *Water Res.* **2006**, *40*, 2776–2786. [CrossRef] [PubMed]
8. Wang, Q.; Cheng, T.; Wu, Y. Distinct roles of illite colloid and humic acid in mediating arsenate transport in water-saturated sand columns. *Water Air Soil Pollut.* **2015**, *226*. [CrossRef]
9. Kretzschmar, R.; Borkovec, M.; Grolimund, D.; Elimelech, M. Mobile subsurface colloids and their role in contaminant transport. *Adv. Agron.* **1999**, *66*, 121–193.
10. Bob, M.M.; Walker, H.W. Effect of natural organic coatings on the polymer-induced coagulation of colloidal particles. *Colloids Surf. A* **2001**, *177*, 215–222. [CrossRef]
11. Franchi, A.; O'Melia, C.R. Effects of natural organic matter and solution chemistry on the deposition and reentrainment of colloids in porous media. *Environ. Sci. Technol.* **2003**, *37*, 1122–1129. [CrossRef] [PubMed]
12. Harbour, P.J.; Dixon, D.R.; Scales, P.J. The role of natural organic matter in suspension stability: Electrokinetic-rheology relationships. *Colloids Surf. A* **2007**, *295*, 38–48. [CrossRef]
13. Laegdsmand, M.; de Jonge, L.W.; Moldrup, P. Leaching of colloids and dissolved organic matter from columns packed with natural soil aggregates. *Soil Sci.* **2005**, *170*, 13–27. [CrossRef]
14. Bekhit, H.M.; Hassan, A.E.; Harris-Burr, R.; Papelis, C. Experimental and numerical investigations of effects of silica colloids on transport of strontium in saturated sand columns. *Environ. Sci. Technol.* **2006**, *40*, 5402–5408. [CrossRef] [PubMed]
15. Saiers, J.E.; Hornberger, G.M. The influence of ionic strength on the facilitated transport of cesium by kaolinite colloids. *Water Resour. Res.* **1999**, *35*, 1713–1727. [CrossRef]
16. Kearns, P.; Gonzalez, M.; Oki, N.; Lee, K.; Rodriguez, F. The safety of nanotechnologies at the oecd. In *Nanomaterials: Risks and Benefits*; Linkov, I., Steevens, J., Eds.; Springer: West Berlin, Germany, 2009; pp. 351–358.
17. Vitorge, E.; Szenknect, S.; Martins, J.M.F.; Barthes, V.; Auger, A.; Renard, O.; Gaudet, J.P. Comparison of three labeled silica nanoparticles used as tracers in transport experiments in porous media, Part I: Syntheses and characterizations. *Environ. Pollut.* **2014**, *184*, 605–612. [CrossRef] [PubMed]
18. Wang, Z.; Zhang, W.J.; Li, S.; Zhou, J.J.; Liu, D. Transport of colloidal silicon through saturated porous media under different hydrogeochemicaland hydrodynamic conditions during managed aquifer recharge. *Water* **2016**, *8*, 555. [CrossRef]
19. Saleh, N.B.; Pfefferle, L.D.; Elimelech, M. Influence of biomacromolecules and humic acid on the aggregation kinetics of single-walled carbon nanotubes. *Environ. Sci. Technol.* **2010**, *44*, 2412–2418. [CrossRef] [PubMed]
20. Chen, K.L.; Elimelech, M. Interaction of fullerene (C60) nanoparticles with humic acid and alginate coated silica surfaces: Measurements, mechanisms, and environmental implications. *Environ. Sci. Technol.* **2008**, *42*, 7607–7614. [CrossRef] [PubMed]
21. Hong, S.; Elimelech, M. Chemical and physical aspects of natural organic matter (NOM) fouling of nanofiltration membranes. *J. Membr. Sci.* **1997**, *132*, 159–181. [CrossRef]

22. Jiang, X.J.; Tong, M.P.; Kim, H. Influence of natural organic matter on the transport and deposition of zinc oxide nanoparticles in saturated porous media. *J. Colloid Interface Sci.* **2012**, *386*, 34–43. [CrossRef] [PubMed]
23. Liu, D.; Zhou, J.J.; Zhang, W.J.; Huan, Y.; Yu, X.P.; Li, F.L.; Chen, X.Q. Column experiments to investigate transport of colloidal humic acid through porous media during managed aquifer recharge. *Hydrol. J.* **2016**. [CrossRef]
24. Syngouna, V.I.; Chrysikopoulos, C.V. Transport of biocolloids in water saturated columns packed with sand: Effect of grain size and pore water velocity. *J. Contam. Hydrol.* **2012**, *129*, 301–314. [CrossRef]
25. Hu, J.D.; Zevi, Y.; Kou, X.M.; Xiao, J.; Wang, X.J.; Jin, Y. Effect of dissolved organic matter on the stability of magnetite nanoparticles under different pH and ionic strength conditions. *Sci. Total Environ.* **2010**, *408*, 3477–3489. [CrossRef] [PubMed]
26. Yang, K.; Lin, D.H.; Xing, B.S. Interactions of humic acid with nanosized inorganic oxides. *Langmuir* **2009**, *25*, 3571–3576. [CrossRef] [PubMed]
27. Jiang, X.J.; Tong, M.P.; Lu, R.Q.; Kim, H. Transport and deposition of ZnO nanoparticles in saturated porous media. *Colloids Surf. A* **2012**, *401*, 29–37. [CrossRef]
28. Torkzaban, S.; Bradford, S.A.; Vanderzalm, J.L.; Patterson, B.M.; Harris, B.; Prommer, H. Colloid release and clogging in porous media: Effects of solution ionic strength and flow velocity. *J. Contam. Hydrol.* **2015**, *181*, 161–171. [CrossRef] [PubMed]
29. Liang, L.; Luo, L.; Zhang, S.Z. Adsorption and desorption of humic and fulvic acids on SiO_2 particles at nano- and micro-scales. *Colloids Surf. A* **2011**, *384*, 126–130. [CrossRef]
30. Chen, G.X.; Liu, X.Y.; Su, C.M. Distinct effects of humic acid on transport and retention of TiO_2 rutile nanoparticles in saturated sand columns. *Environ. Sci. Technol.* **2012**, *46*, 7142–7150. [CrossRef] [PubMed]
31. Ben-Moshe, T.; Dror, I.; Berkowitz, B. Transport of metal oxide nanoparticles in saturated porous media. *Chemosphere* **2010**, *81*, 387–393. [CrossRef] [PubMed]
32. Thio, B.J.R.; Zhou, D.X.; Keller, A.A. Influence of natural organic matter on the aggregation and deposition of titanium dioxide nanoparticles. *J. Hazard. Mater.* **2011**, *189*, 556–563. [CrossRef] [PubMed]
33. Li, K.G.; Chen, Y.S. Effect of natural organic matter on the aggregation kinetics of CeO_2 nanoparticles in KCl and $CaCl_2$ solutions: Measurements and modeling. *J. Hazard. Mater.* **2012**, *209*, 264–270. [CrossRef] [PubMed]
34. Anderson, B.J. University of Birmingham, Birmingham, England. The mobility of colloids in red sandstone: The effect of flow rate and ionic strength. Unpublished work, 2008.
35. Elimelech, M.; Nagai, M.; Ko, C.H.; Ryan, J.N. Relative insignificance of mineral grain zeta potential to colloid transport in geochemically heterogeneous porous media. *Environ. Sci. Technol.* **2000**, *34*, 2143–2148. [CrossRef]